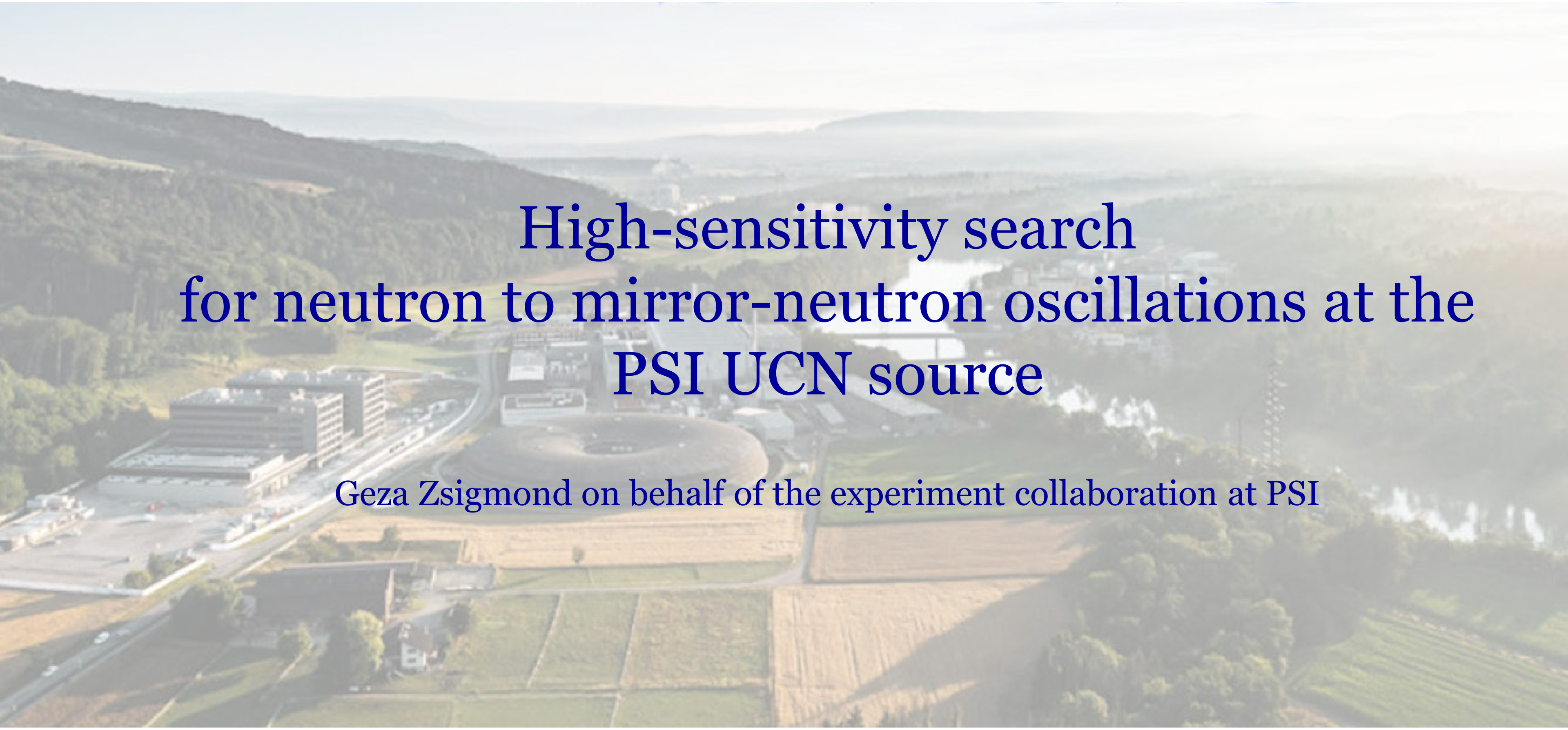

High-sensitivity search for neutron to mirror-neutron oscillations at the PSI UCN source

Geza Zsigmond on behalf of the experiment collaboration at PSI

Experiment collaboration

New high-sensitivity search for neutron to mirror-neutron oscillations at the PSI UCN source

N. J. Ayres,[1] Z. Berezhiani,[2] G. Bison,[3] K. Bodek,[4] V. Bondar,[1] P.-J. Chiu,[1,3,*] M. Daum,[3] C. B. Doorenbos,[1,3] S. Emmenegger,[1] K. Kirch,[1,3] V. Kletzl,[1,3,†] J. Krempel,[1] B. Lauss,[3,‡] D. Pais,[1,3] I. Rienäcker,[3] D. Ries,[3] D. Rozpędzik,[4] P. Schmidt-Wellenburg,[3] K. S. Tanaka,[3,§] J. Zejma,[4] N. Ziehl,[1,¶] and G. Zsigmond[3,‖]

[1]*Institute for Particle Physics and Astrophysics, ETH Zürich, 8093 Zürich, Switzerland*
[2]*INFN, Laboratori Nazionali del Gran Sasso, Assergi, 67100 L'Aquila, Italy*
[3]*Laboratory for Particle Physics, PSI Center for Neutron and Muon Sciences, Paul Scherrer Institute (PSI), 5232 Villigen, Switzerland*
[4]*Marian Smoluchowski Institute of Physics, Jagiellonian University, 30-348 Cracow, Poland*

In a search for potential signals of neutron (n) to mirror-neutron (n') oscillations, a collaboration centered at the Paul Scherrer Institute (PSI) investigated the remaining parameter space claimed by anomalies with a dedicated high-sensitivity apparatus. An elaborate magnetic-field-mapping analysis and Monte Carlo simulation of the cumulative $n-n'$ oscillation probabilities along the neutron trajectories inside the storage vessel complemented the neutron data analysis. Magnetic fields were scanned in the range $5\,\mu\mathrm{T} < B < 109\,\mu\mathrm{T}$. No evidence of anomalous neutron losses was found. Consequently, new limits for the $n-n'$ oscillation time constant were set. The parameter space, previously claimed for potential signals, has been excluded to 99.98 %.

Mass-degenerate analysis: Phys. Rev. Lett. **137**, 051802 (2026);
arXiv:2602.23487
Finite-splitting analysis: arXiv:2608.12173 (2026)

Mirror matter

- A parallel mirror sector of particles as an exact duplicate of the ordinary particle sector was proposed a long time ago to restore parity symmetry on a global level in the weak interaction [1–4].
- Ordinary particles: the electron e, proton p, neutron n etc., have mass degenerate mirror partners: e′, p′, n′ etc. which are sterile to our Standard Model interactions.
- Besides gravity, mirror particles can interact with ordinary matter only via specific feeble interactions [5, 6].
- Neutral particle to mirror particle oscillations, as n→n′ with $\tau_{nn'} > 1$ s.
- Mirror matter could account for dark matter, provided that during the evolution of the Universe it had a lower temperature than the ordinary sector [7–10].

[1] T. D. Lee and C.-N. Yang, Phys. Rev. 104, 254 (1956).
[2] I. Y. Kobzarev, L. B. Okun, and I. Y. Pomeranchuk, Sov. J. Nucl. Phys. 3, 837 (1966).
[3] S. I. Blinnikov and M. Khlopov, Sov. Astron. 27, 371 (1983).
[4] R. Foot and R. R. Volkas, Phys. Rev. D 68, 021304 (2003).
[5] Z. Berezhiani, Int. J. Mod. Phys. A 19, 3775 (2004)
[6] R. Foot, Int. J. Mod. Phys. A 19, 3807 (2004)
[7] Z. Berezhiani, D. Comelli, and F. L. Villante, Phys. Lett. B 503, 362 (2001)
[8] A. Y. Ignatiev and R. R. Volkas, Phys. Rev. D 68, 023518 (2003)
[9] Z. Berezhiani, P. Ciarcelluti, D. Comelli, and F. L. Villante, Int. J. Mod. Phys. D 14, 107 (2005)
[10] Z. Berezhiani, S. Cassisi, P. Ciarcelluti, and A. Pietrinferni, Astropart. Phys. 24, 495 (2006)

Mass-degenerate case with a mirror field B′

- Exact mirror parity predicts $m_n = m_{n'}$. A hypothetical local B′ changes the mirror-neutron Zeeman energy and hence the relative level splitting.
- Conversion is enhanced near B ≃ ±B′. The sterile n′ component is not confined by ordinary material walls and appears as an additional UCN loss.

$$H_I = \begin{pmatrix} \mu_n \mathbf{B}\cdot\boldsymbol{\sigma} & \varepsilon_{nn'}\,\mathbf{1} \\ \varepsilon_{nn'}\,\mathbf{1} & \mu_n \mathbf{B}'\cdot\boldsymbol{\sigma} \end{pmatrix} \qquad \tau_{nn'} = \frac{1}{\varepsilon_{nn'}} \quad (\hbar = c = 1)$$

I. Rienaecker, ETH Zurich PhD thesis (2022), Eq. (1.30).

hypothetical local mirror field

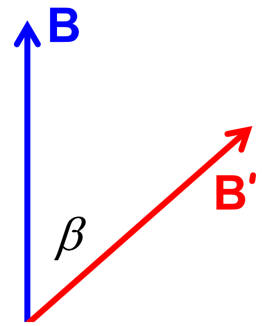

$$P^{nn'}_{BB'}(t) = \frac{\sin^2[(\omega-\omega')t]}{2\tau^2_{nn'}(\omega-\omega')^2} + \frac{\sin^2[(\omega+\omega')t]}{2\tau^2_{nn'}(\omega+\omega')^2} + \left(\frac{\sin^2[(\omega-\omega')t]}{2\tau^2_{nn'}(\omega-\omega')^2} - \frac{\sin^2[(\omega+\omega')t]}{2\tau^2_{nn'}(\omega+\omega')^2}\right)\cos\beta$$

$$\omega = |\mu_n B|/2\hbar \text{ and } \omega' = |\mu_n B'|/2\hbar$$

Resonant enhancement

for B ≃ B′ or B ≃ −B′

Z. Berezhiani and F. Nesti, Eur. Phys. J. C 72, 1974 (2012).

Previously reported UCN loss anomalies

- Several earlier UCN experiments performed by other groups at different magnetic-field settings reported deviations from the null hypothesis: 2.5σ, 3σ and 5σ effects.
- **These claims motivated a dedicated search with substantially improved sensitivity.**

$$\tau_{nn'} = \hbar \varepsilon^{-1}$$

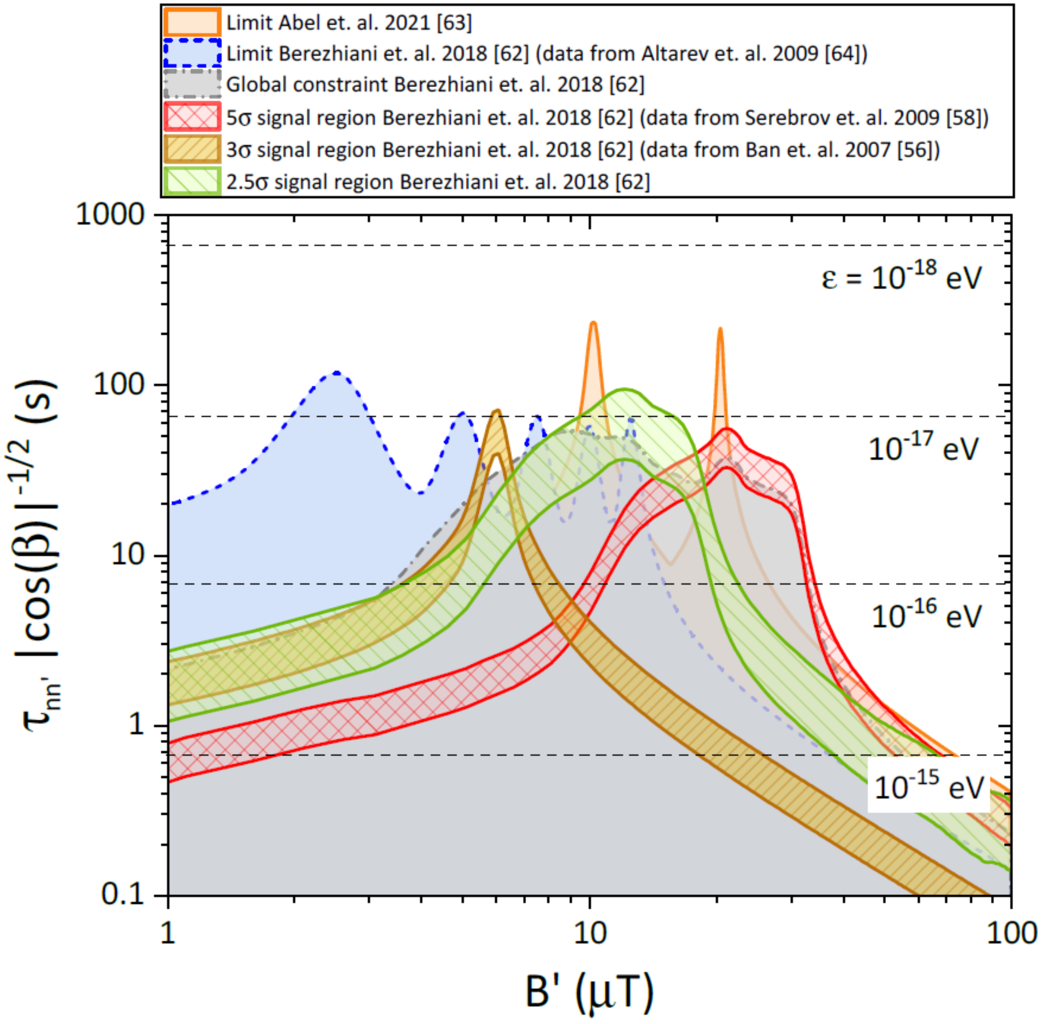

Ultracold neutrons and UCN source at PSI

Ultracold – storable neutrons (UCN)

Total reflection at any incident angle – material dependent Ni, Ni[58], Be, DLC, steel

V_F = 150 - 300 neV

(neutron optical potential)

UCN (< 260 neV) **< 7 m/s** **> 500 Å**

magnetic

$V_m = -\mu B$

60 neV T^{-1}

gravity

$V_g = m_n g h$

100 neV m^{-1}

UCN density profile

UCN storage/observation times: hundreds of seconds

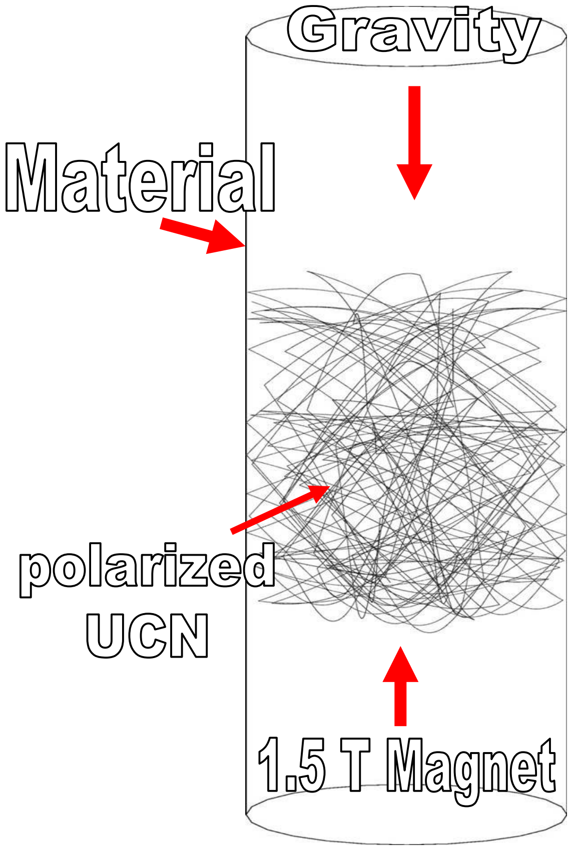

Neutron reflection on walls

Quantum reflection on or transmission through an average nucleus-neutron potential

$$U = V - iW = \frac{2\pi\hbar^2}{m} N\left(b_{coh} - i\frac{\sigma_l k}{4\pi}\right)$$

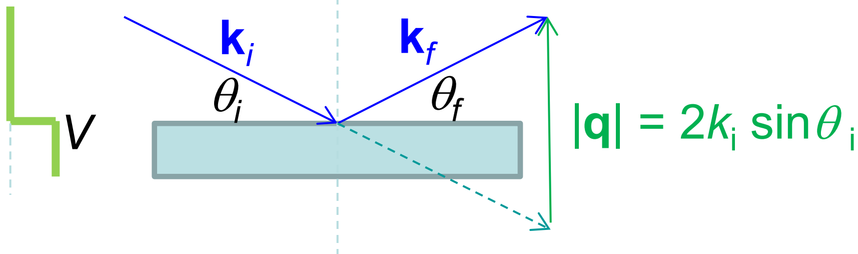

$$E_{i\perp} = \frac{(\hbar k_i \sin\theta_i)^2}{2m}$$

$$\left(\frac{q}{q_c}\right)^2 = \frac{E_\perp}{V}$$

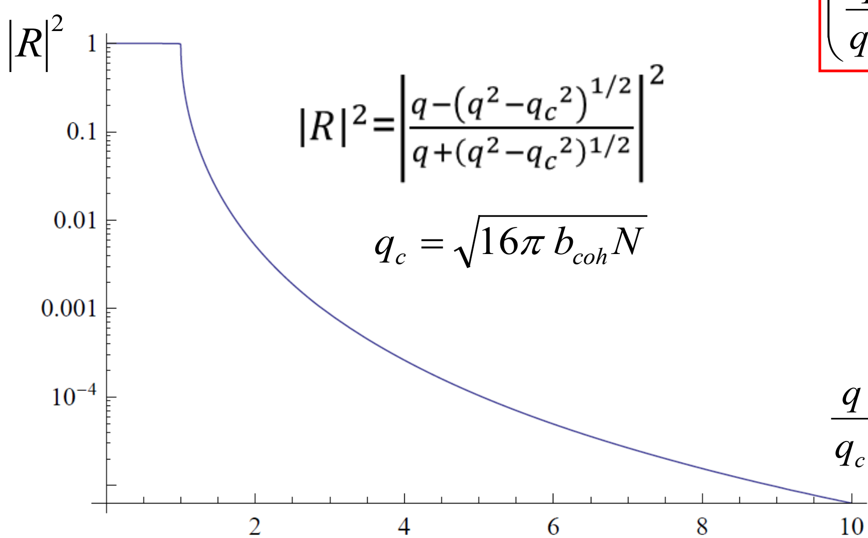

$$|R|^2 = \left|\frac{q-(q^2-q_c^2)^{1/2}}{q+(q^2-q_c^2)^{1/2}}\right|^2$$

$$q_c = \sqrt{16\pi\, b_{coh} N}$$

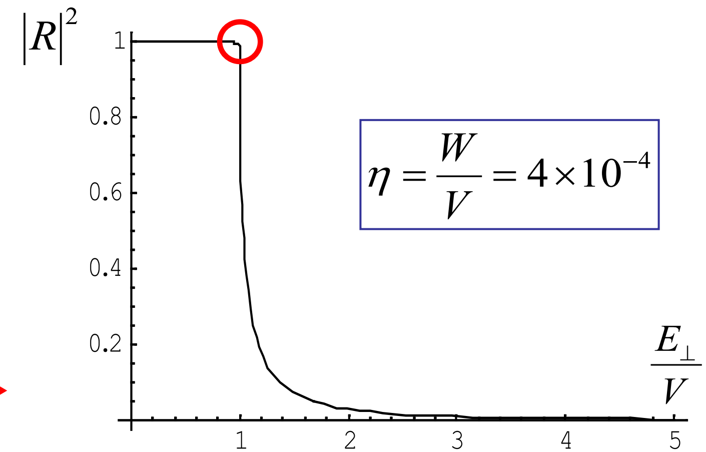

$$\eta = \frac{W}{V} = 4\times 10^{-4}$$

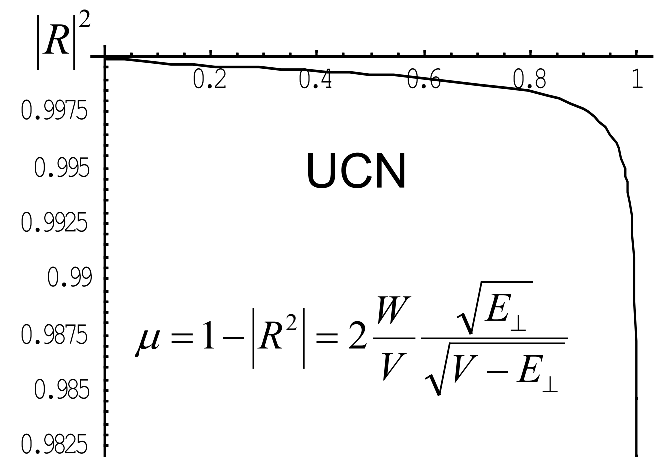

$$\mu = 1 - \left|R^2\right| = 2\frac{W}{V}\frac{\sqrt{E_\perp}}{\sqrt{V - E_\perp}}$$

Ultracold neutron source at PSI

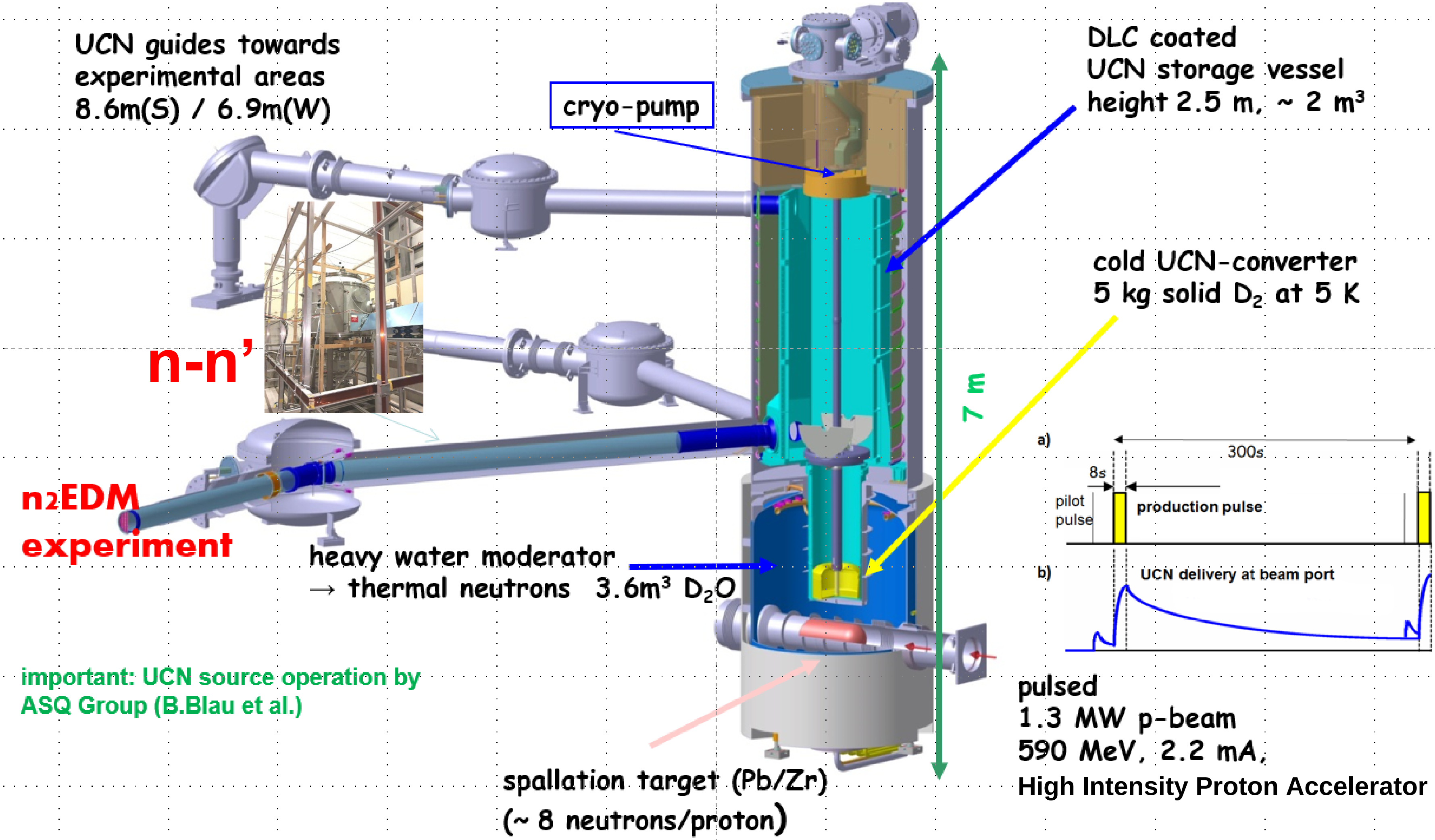

important: UCN source operation by ASQ Group (B.Blau et al.)

Benchmark of the UCN source MCUCN model

- n2EDM model includes the PSI source, benchmarked up to the beamport (BP) with various test measurements
  - UCN transmission from BP West-1 to South after pre-storage – constrain loss and diffuse reflection parameters of the guides
  - UCN storage at different heights above BP level – constrain the energy spectrum exiting the sD2
  - TOF spectra at BP,
    foil and guide transmissions
- Global benchmark Eur. Phys. J. A (2022)
  see also Eur. Phys. J. A 56, 33 (2020)

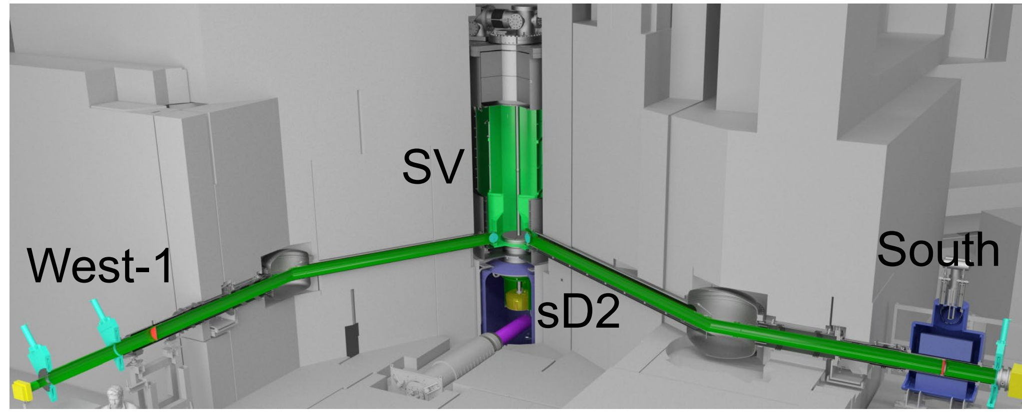

Phys. Rev. C 95 045503 (2017)

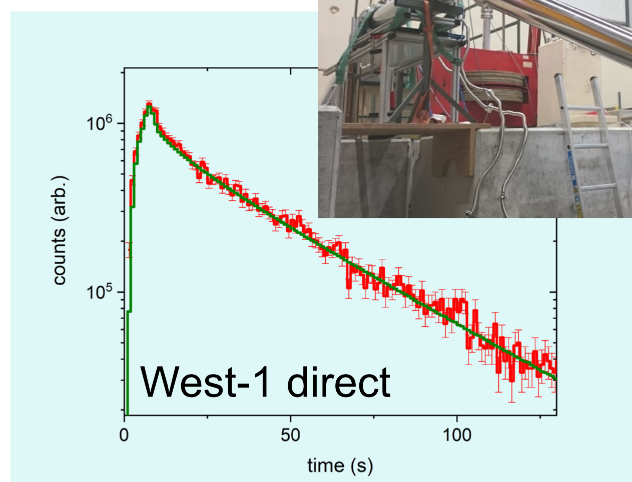

Experimental set-up and MC benchmarks

n-n′ experiment set-up at PSI

Store UCNs for a long observation time:

accumulate n-n’ oscillation probability

n-n′ experiment view from the top

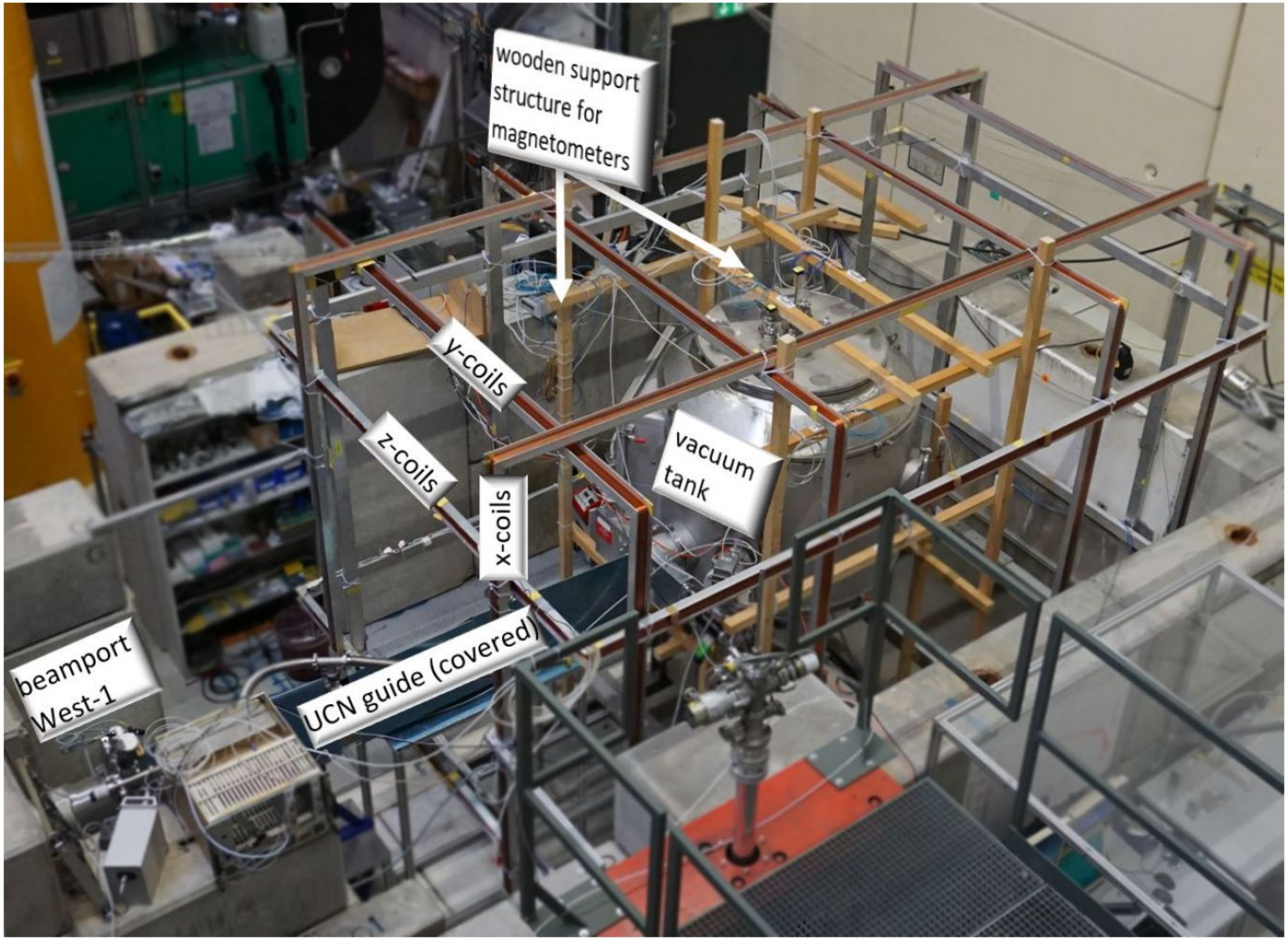

Experiment components and measurement steps

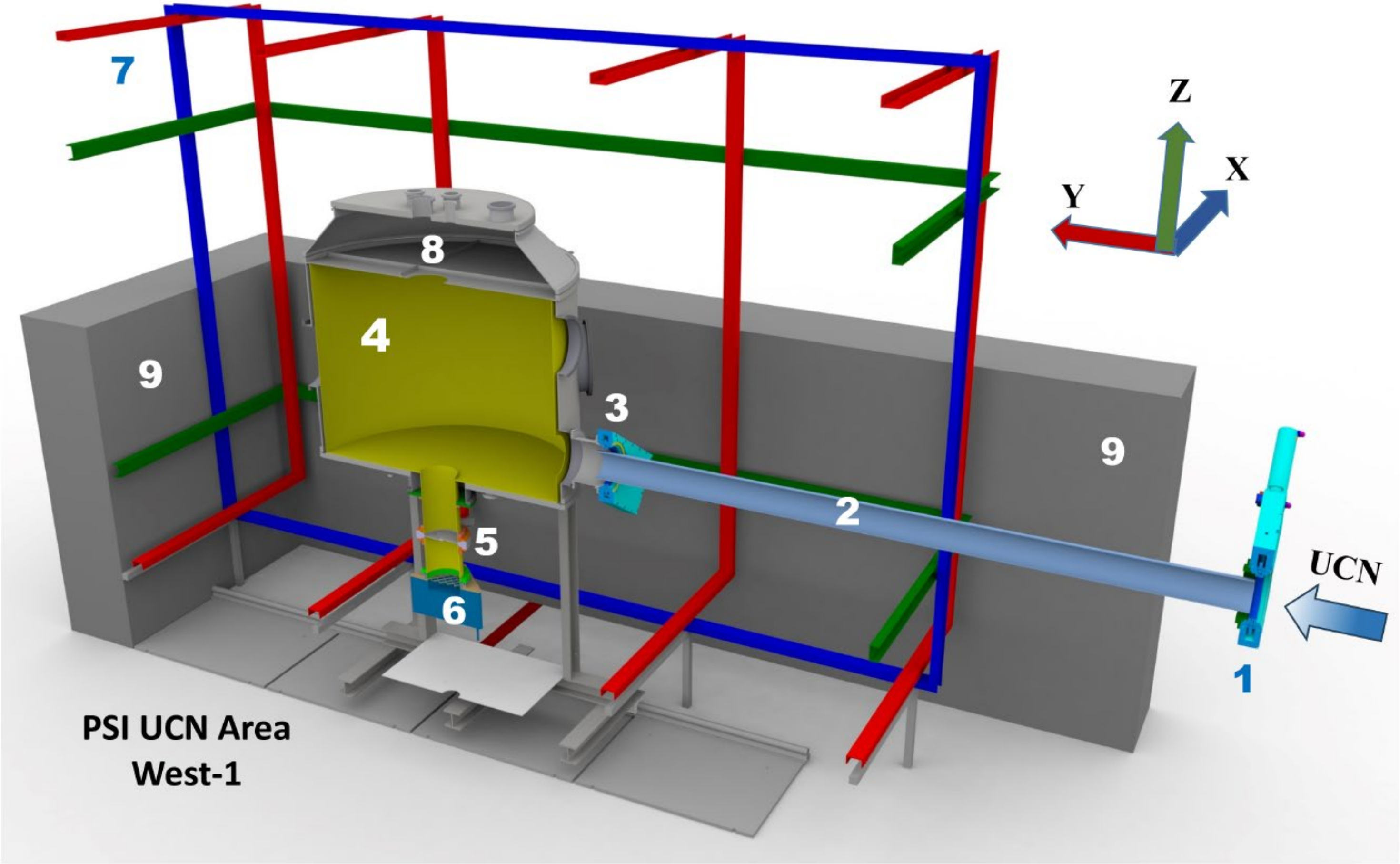

(1) West-1 beamport shutter, (2) UCN guides, (3) horizontal guide shutter, (4) storage vessel, (5) butterfly shutter, (6) UCN detector, (7) magnetic field coils, (8) top lid of the storage vessel, (9) radiation shielding.

Measurement cycle intervals

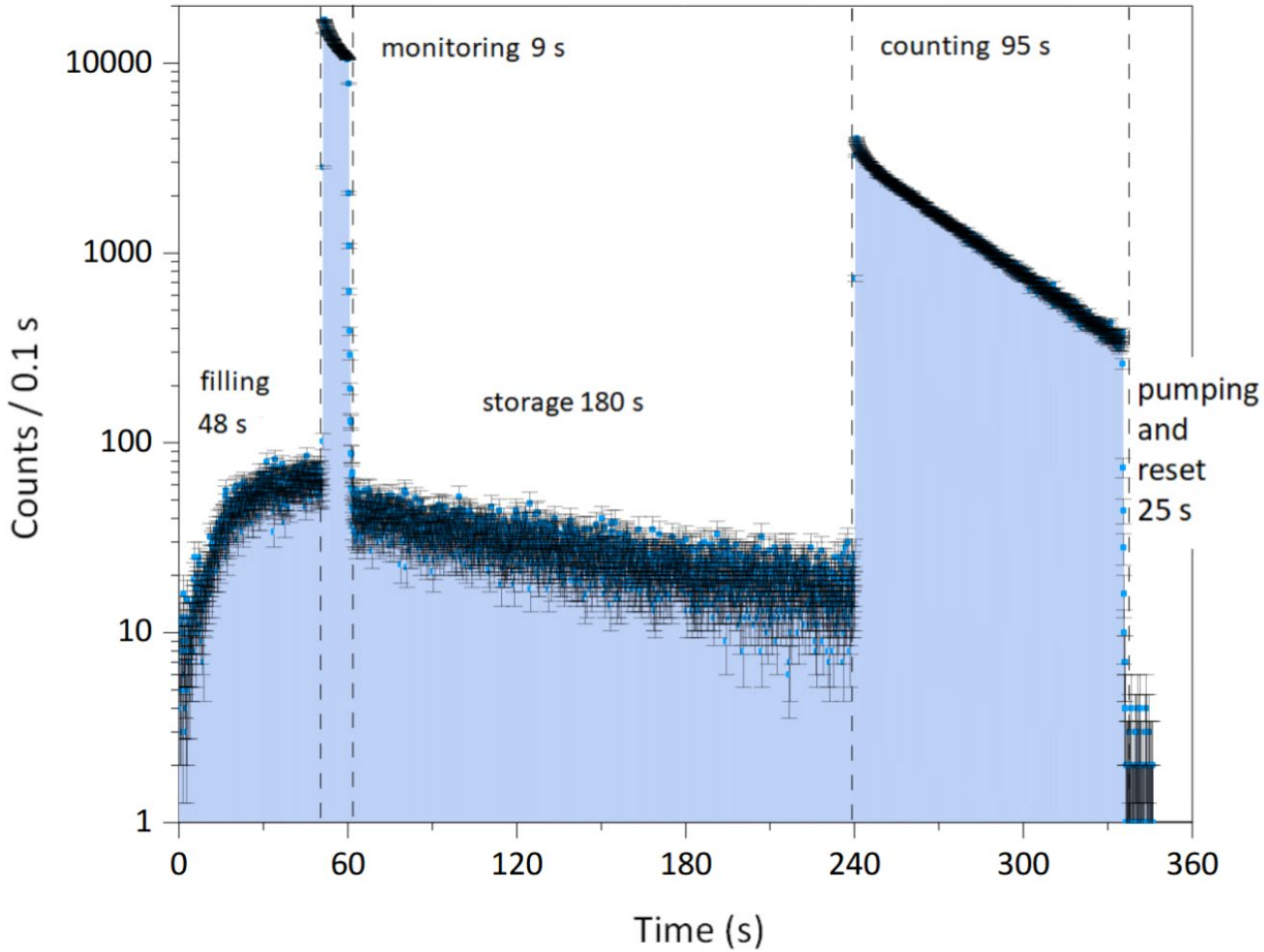

MCUCN ray-tracing model

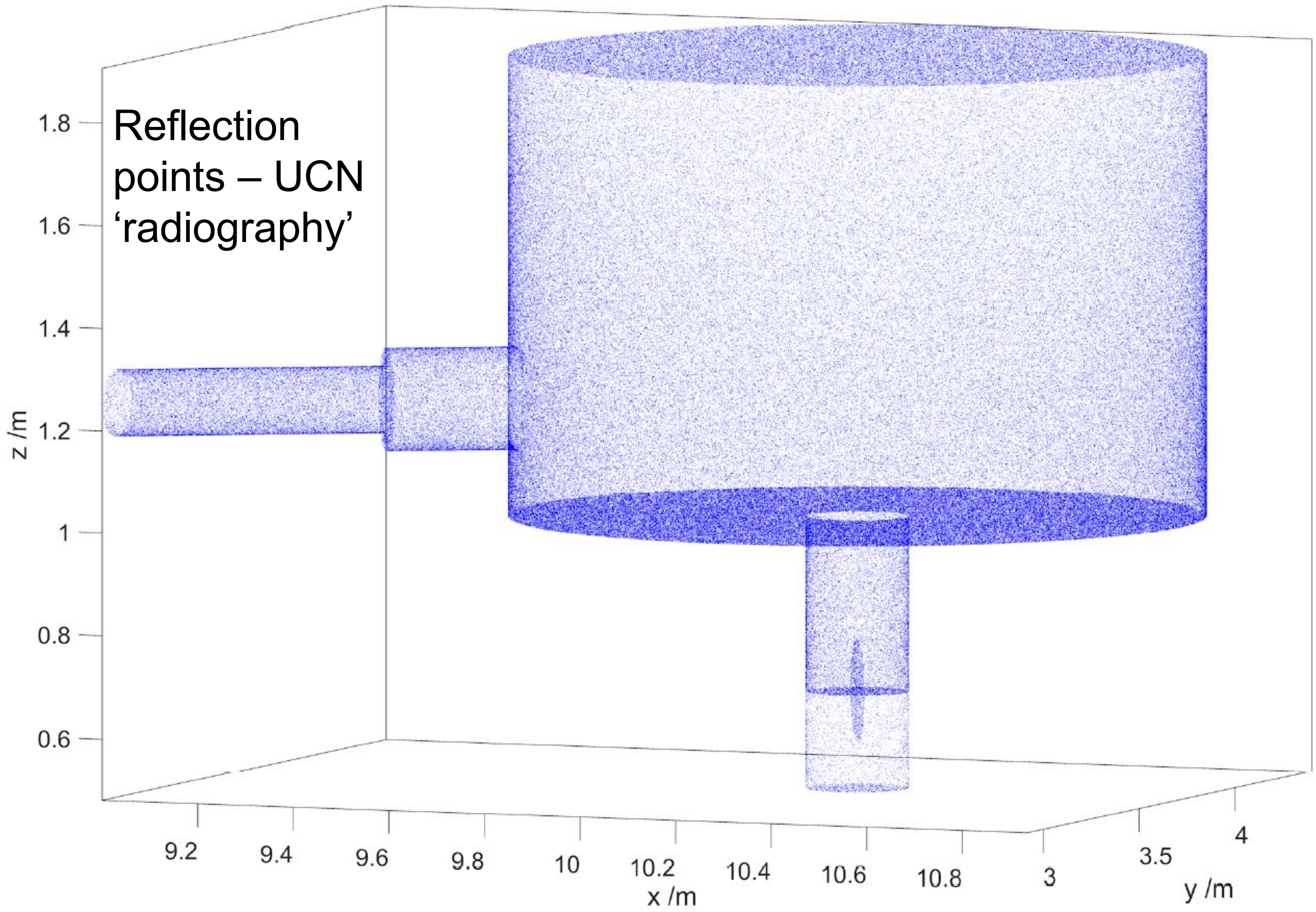

Tuning of the MCUCN model parameters

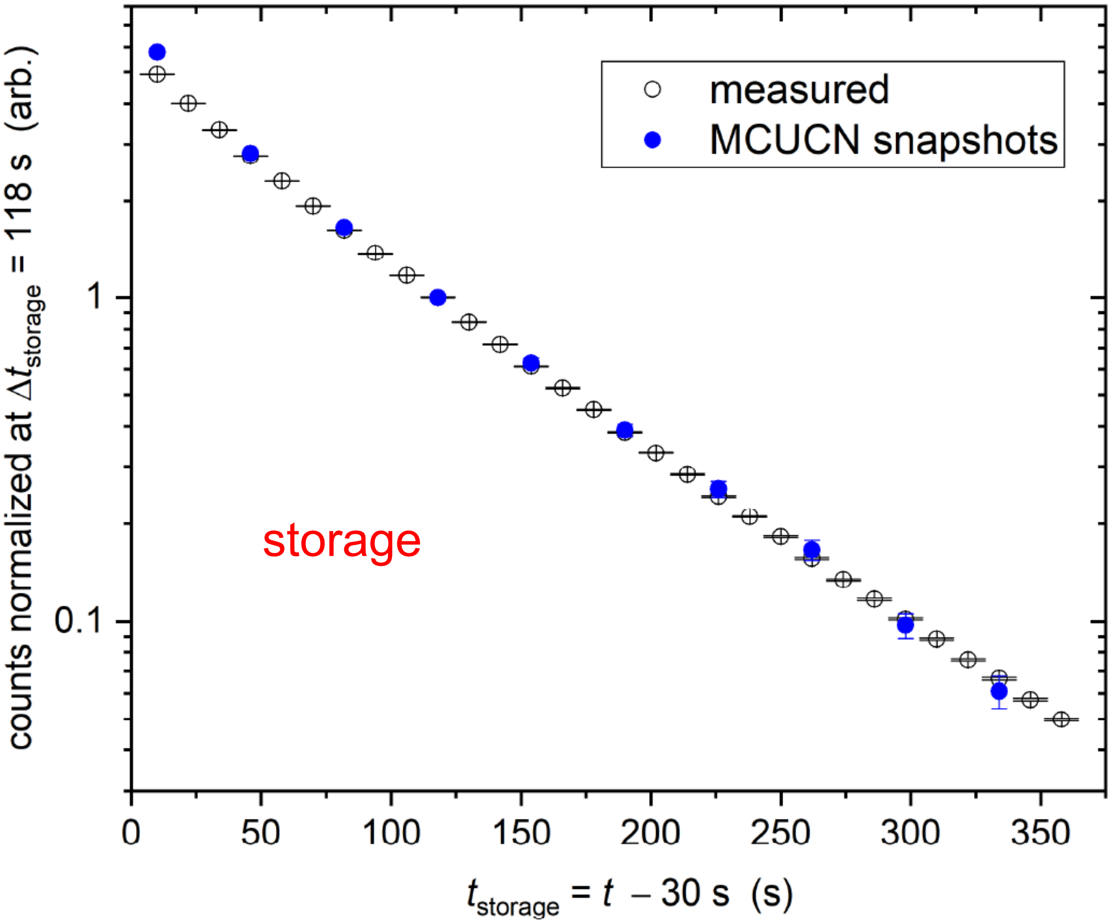

Test of the MCUCN model parameters

No tuning here!

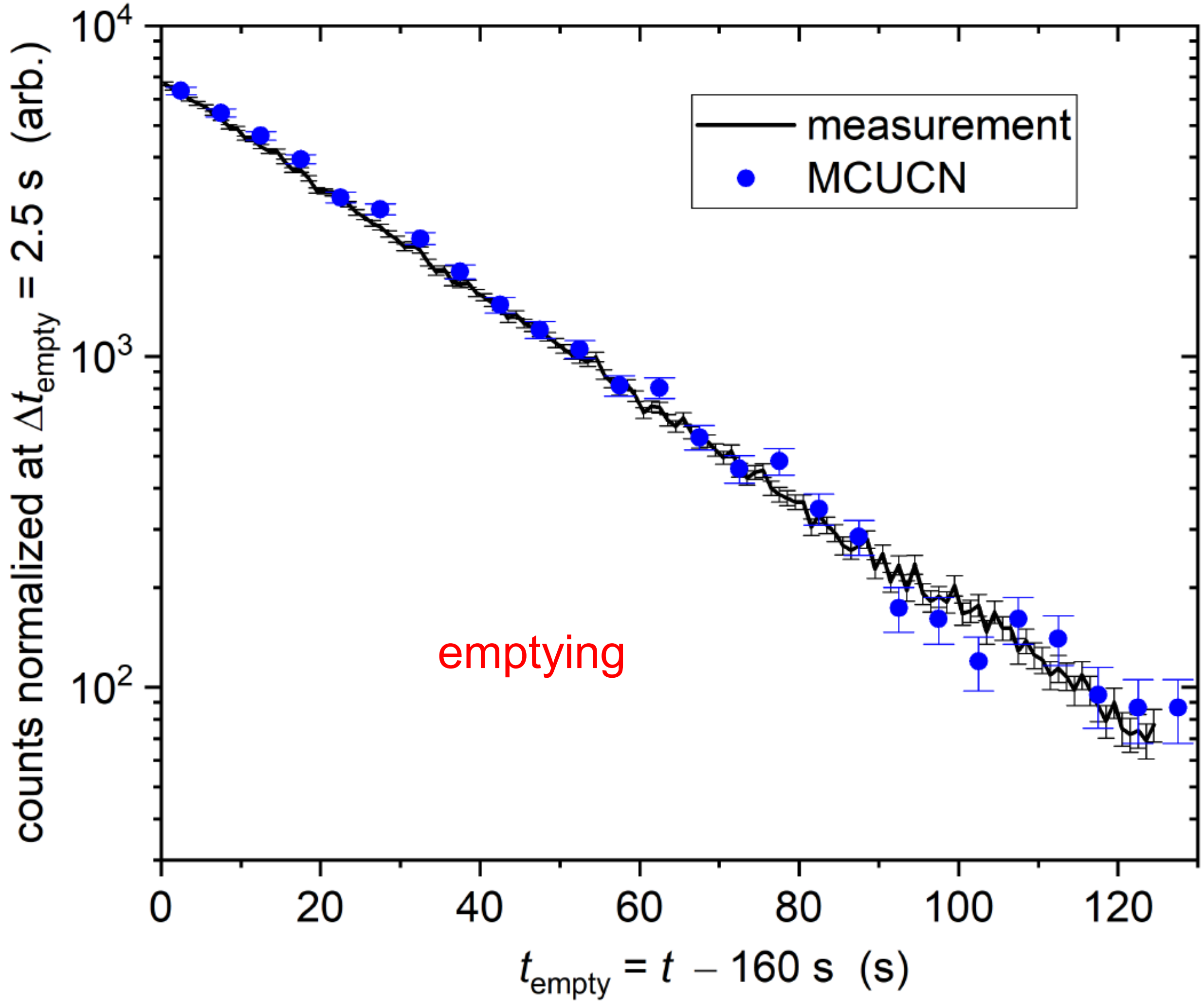

Data analysis: oscillation limits

Asymmetry as observable

Best sensitivity: A = field up, B = field down

(linear drifts in the UCN source: ABBA BAAB sequences)

$$A_j^B = \frac{\sum_i n_{A,i} - \sum_i n_{B,i}}{\sum_i n_{A,i} + \sum_i n_{B,i}}$$

Equate observable with ratio calculated from MCUCN

$$A_B = \frac{n_B^{(t_s)} - n_{-B}^{(t_s)}}{n_B^{(t_s)} + n_{-B}^{(t_s)}} = \frac{\exp(-m_s P_{BB'}^{nn'}) - \exp(-m_s P_{-BB'}^{nn'})}{\exp(-m_s P_{BB'}^{nn'}) + \exp(-m_s P_{-BB'}^{nn'})}$$

UCN counts MC simulations using mag. fields

Search for anomalous losses

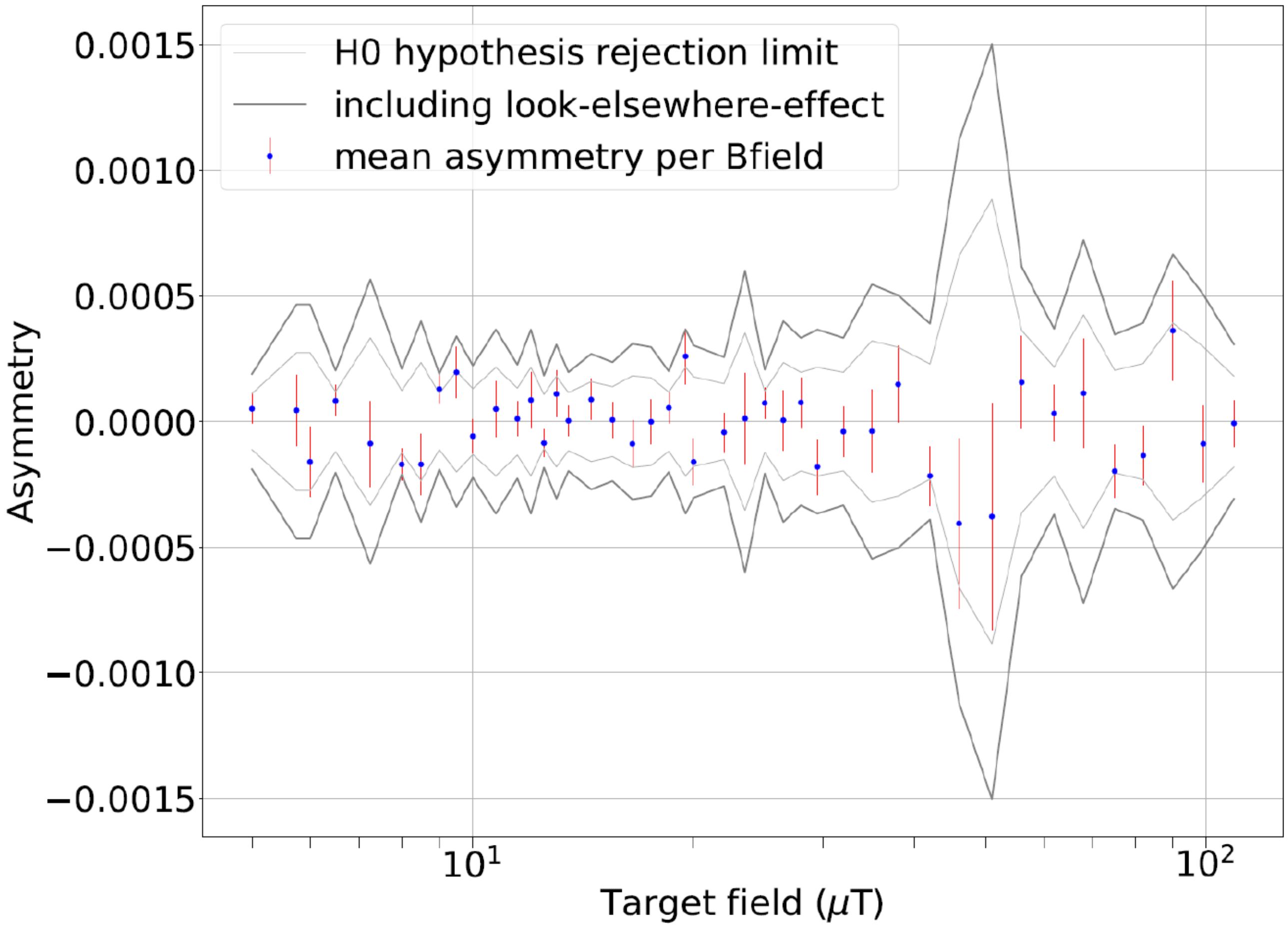

Mean asymmetry ⟨ A_B ⟩ as a function of target field B. The light grey line shows the limits of the null-hypothesis H0 at the 95% C.L., the dark grey outline shows the same limit after correcting for the look-elsewhere-effect. ⟨ A_B ⟩ is consistent with H0 within a standard error δ⟨A_B⟩.

Magnetic field mapping – input for MCUCN

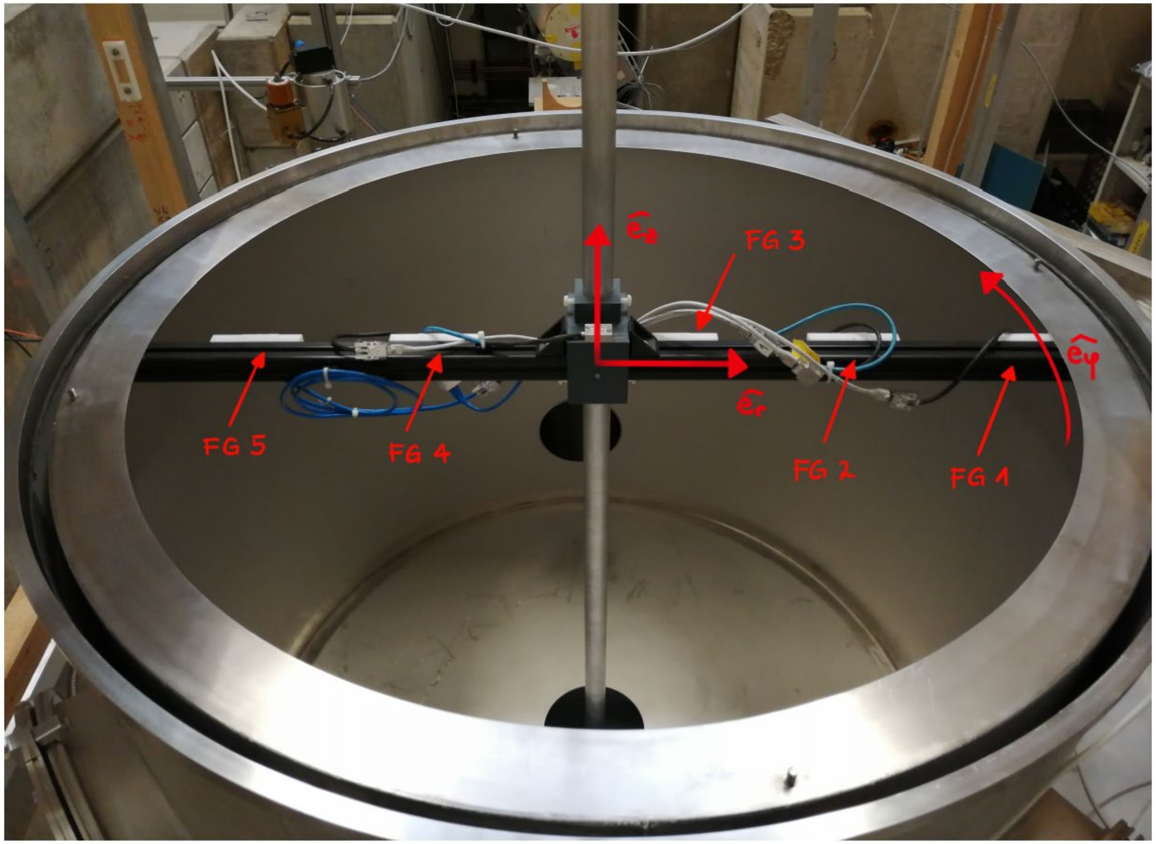

Decompose B-field in harmonic polynomials: $$\mathbf{B}(\mathbf{r}) = \sum_{l,m} G_{l,m}\Pi_{l,m}(\mathbf{r})$$

Mirror field parametrization and the oscillation time parameter

PSI

$$\mathbf{B}' = B' \begin{pmatrix} \sin b \cos a \\ \sin b \sin a \\ \cos b \end{pmatrix}, \mathbf{B} = B(\mathbf{x}) \begin{pmatrix} \sin\theta(\mathbf{x}) \cos\phi(\mathbf{x}) \\ \sin\theta(\mathbf{x}) \sin\phi(\mathbf{x}) \\ \cos\theta(\mathbf{x}) \end{pmatrix}$$

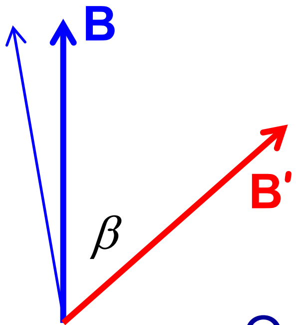

$$\cos(\beta(\mathbf{x})) = \sin b \cos a \sin\theta \cos\phi + \sin b \sin a \sin\theta \sin\phi + \cos b \cos\theta$$

Inhomogeneous field

Oscillation time constant from ‘resonance functions’ (MCUCN)

$$\tau_{nn'} = \frac{1}{\sqrt{2|\langle A_B \rangle|}} \left| F_A^0(\mathbf{B}, B') + F_A^1(\mathbf{B}, B') \cos b + F_A^2(\mathbf{B}, B') \sin b \cos a + F_A^3(\mathbf{B}, B') \sin b \sin a \right|^{\frac{1}{2}}$$

Resampling the $\langle A_B \rangle$, $\delta\langle A_B\rangle$ asymmetry distribution

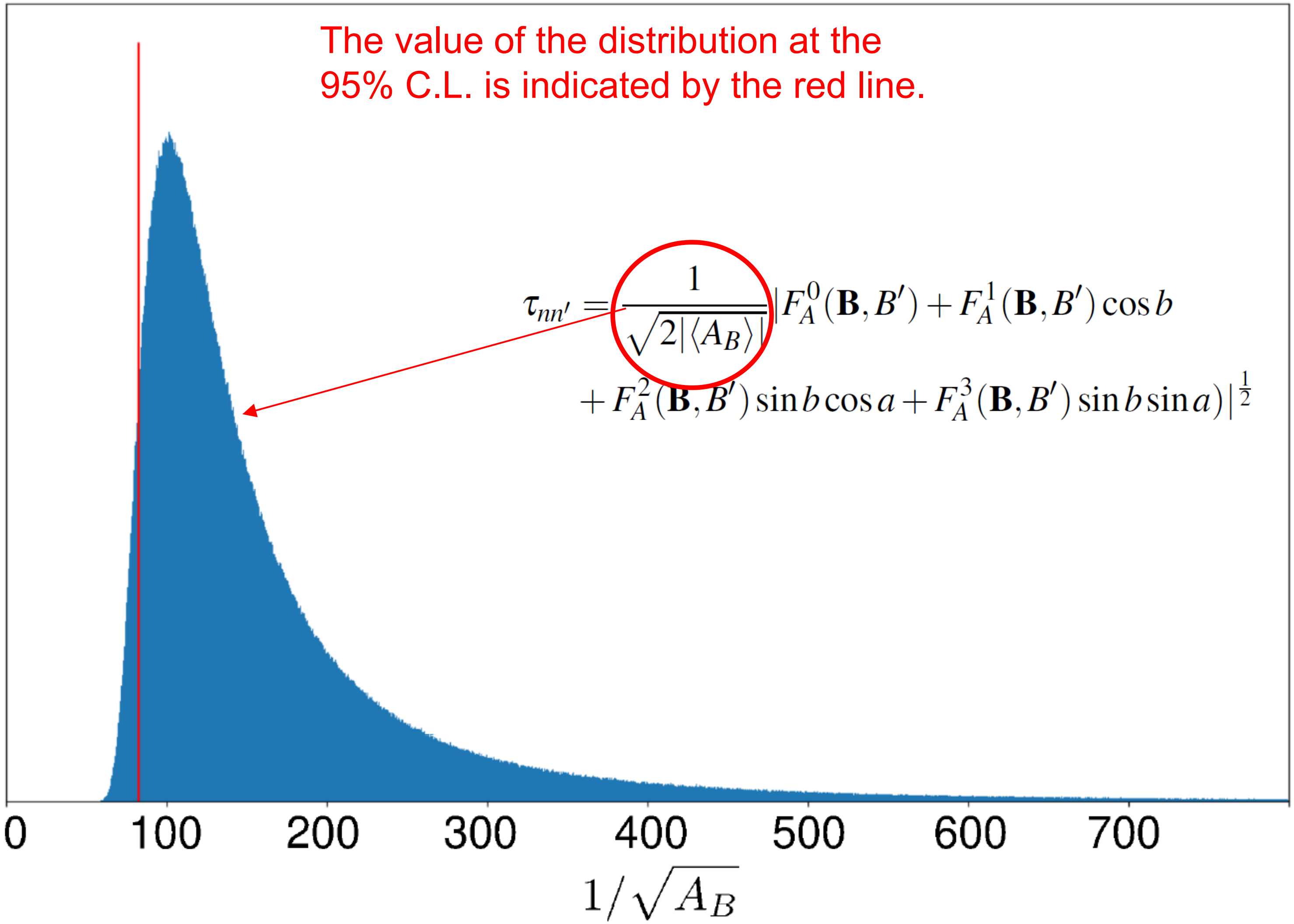

Example resonance functions from MCUCN

$$\tau_{nn'} = \frac{1}{\sqrt{2|\langle A_B\rangle|}} |F_A^0(\mathbf{B},B') + F_A^1(\mathbf{B},B')\cos b + F_A^2(\mathbf{B},B')\sin b\cos a + F_A^3(\mathbf{B},B')\sin b\sin a)|^{\frac{1}{2}}$$

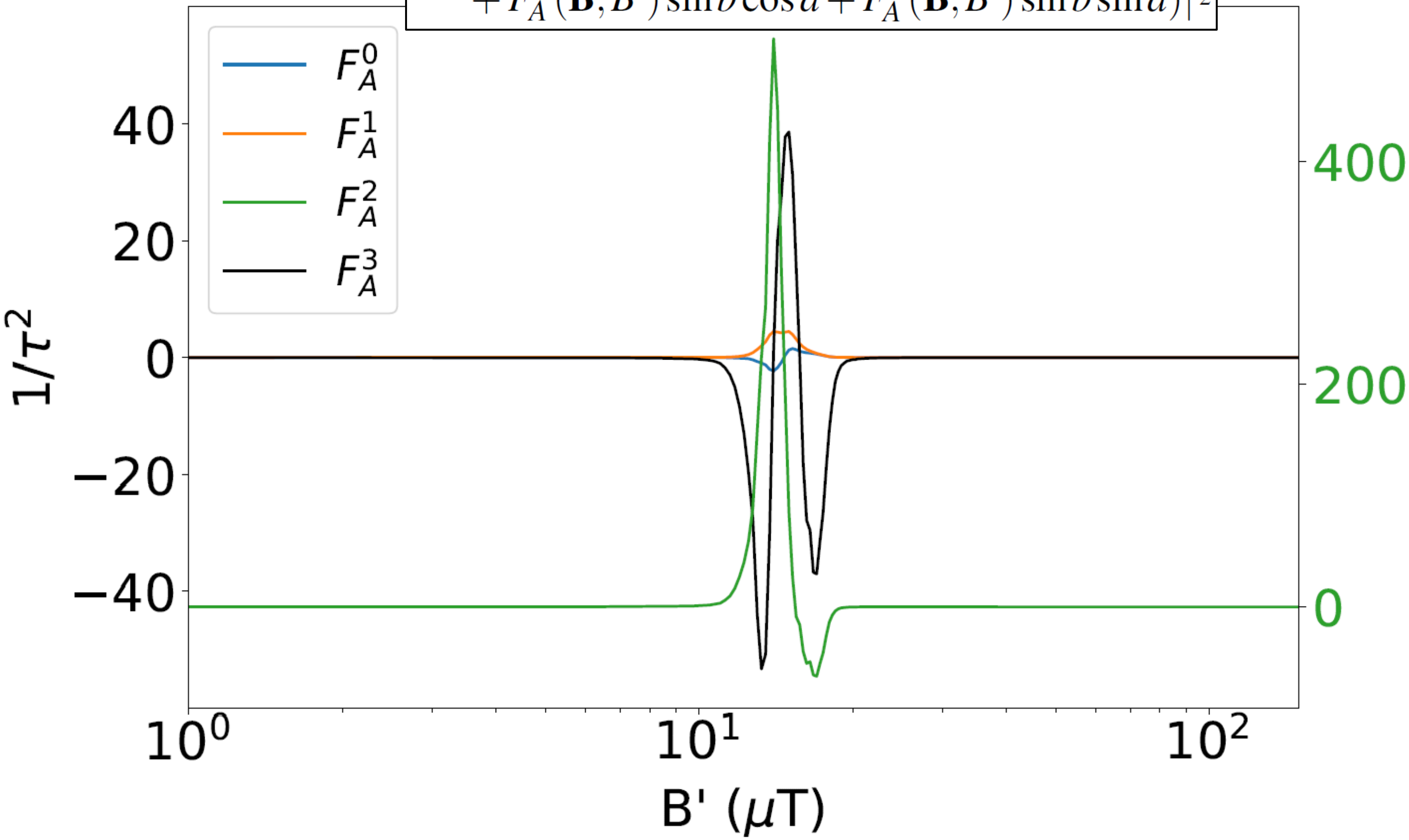

Target magnetic field |B| = 12 μT

Target B-field and limits

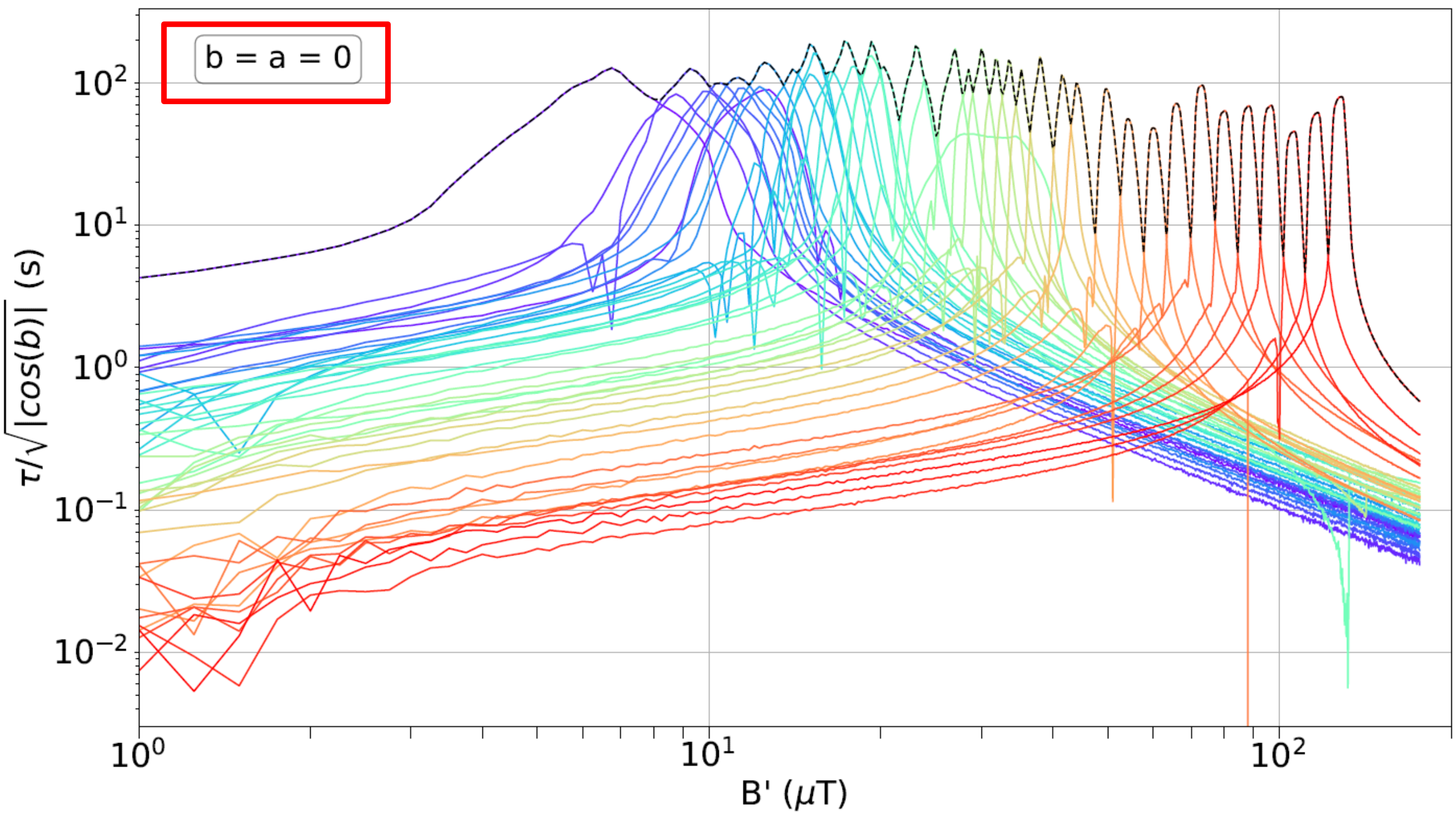

Limits on the oscillation time for all different target fields |B|.
The overall limit is obtained by taking the upper envelope of all (dashed black line).

Dependence of the B' directional parameters

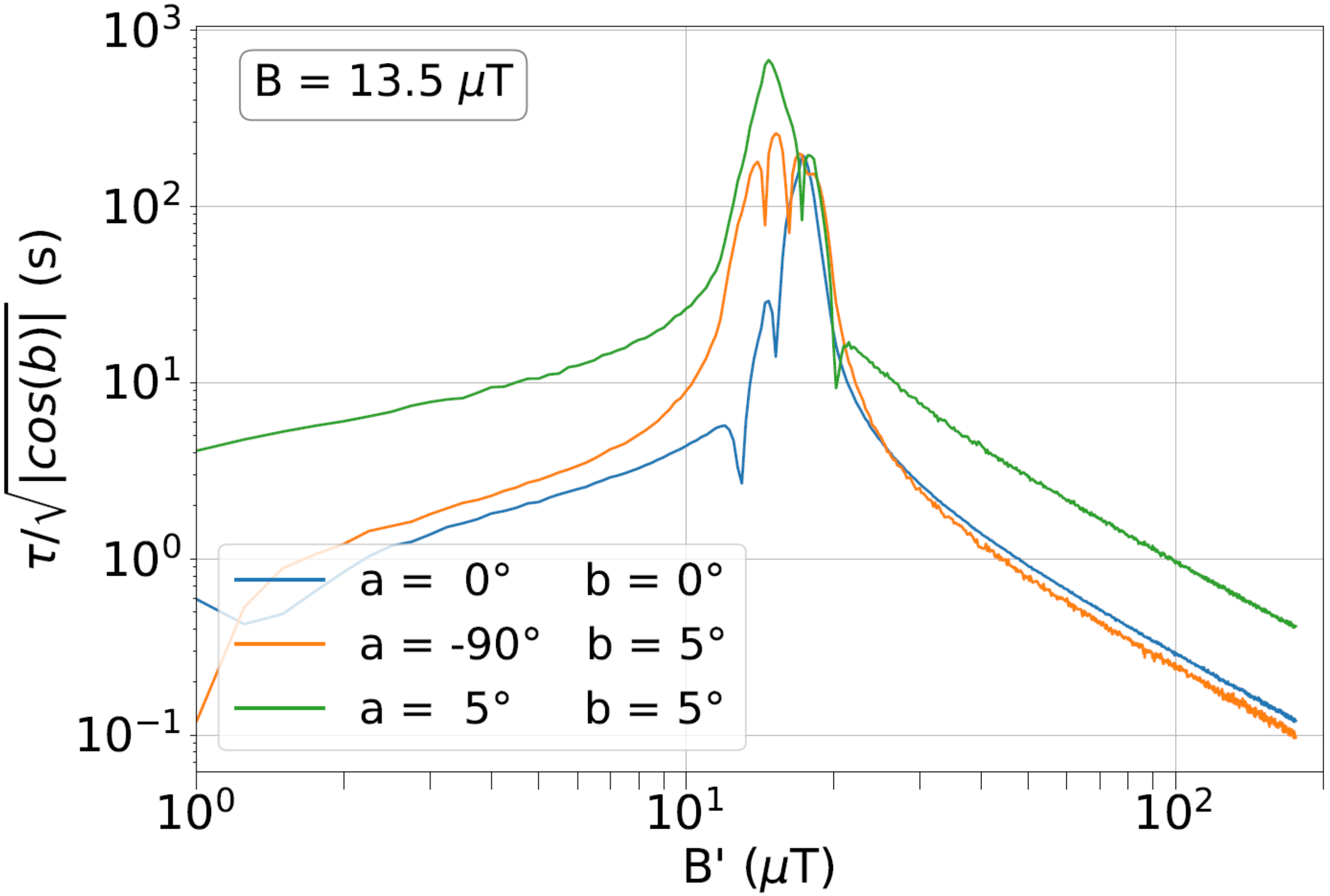

Example limits of $\tau_{nn'}$ at |B| = 13.5 µT, demonstrating the effect of the direction of **B**′.

Oscillation time limits at 95% C.L.

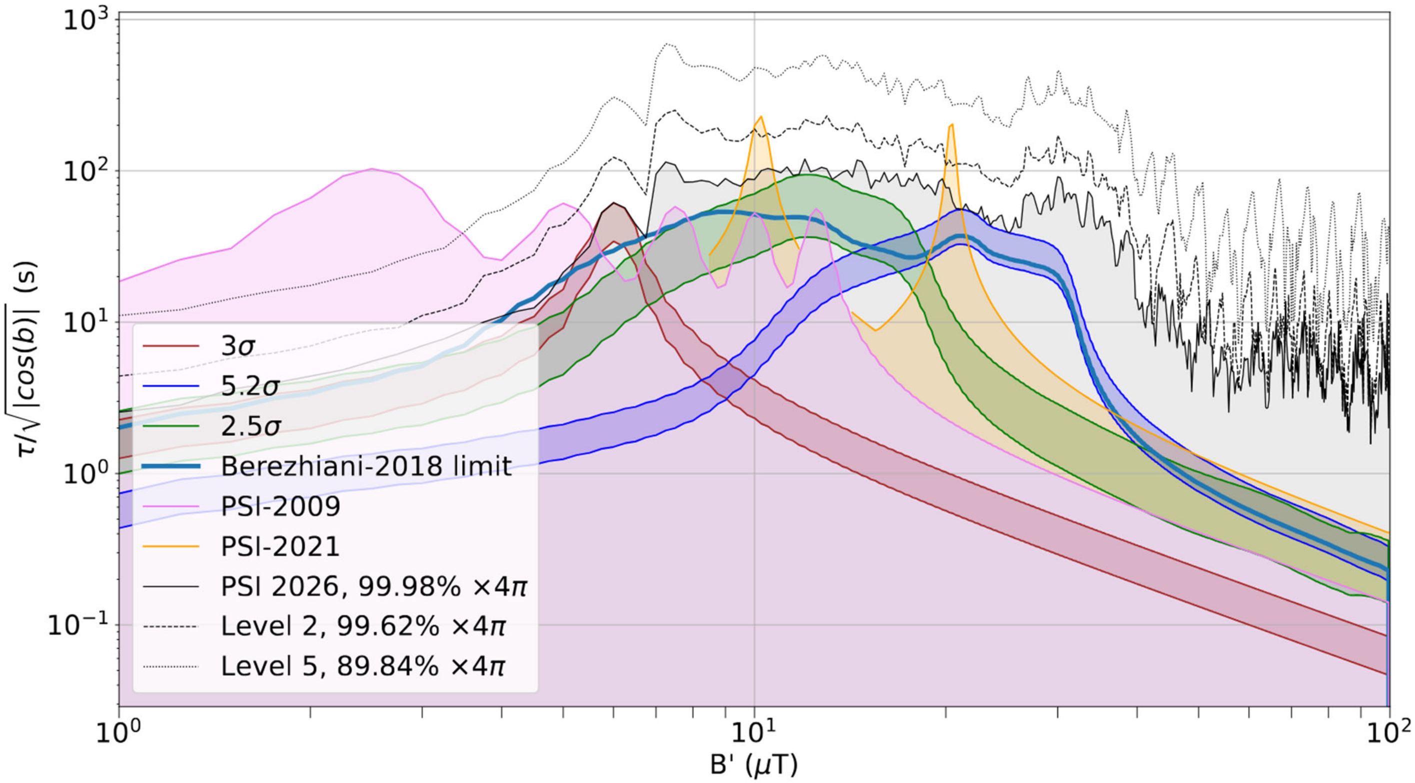

The anomalous signal regions of Berezhiani-2018 [42] from data in [37] (3σ, red), [40] (5.2σ, blue), and [42] (2.5σ, green) together with the 95% CL limits on $\tau_{nn'}/\sqrt{|\cos(b)|}$ from PSI-2009 [41], PSI-2021 [43], and this Letter as a function of the magnitude of the mirror magnetic field B′. Along with the most conservative PSI-2026 limit (black line) excluding 99.98% of the full solid angle (4π) defined in the (a, b) parameter space, two higher limit curves but with less solid angle exclusion (99.62% and 89.84%) are plotted, corresponding to levels of factor 2 (dashed line) and 5 (dotted line) above the anomalous signals.

N. J. Ayres et al., "New High-Sensitivity Search for Neutron to Mirror-Neutron Oscillations at the PSI Ultracold Neutron Source," Phys. Rev. Lett. 137, 051802 (2026), DOI: 10.1103/2qck-n6mb (CC BY 4.0).

Overall dependence of the B' directional parameters

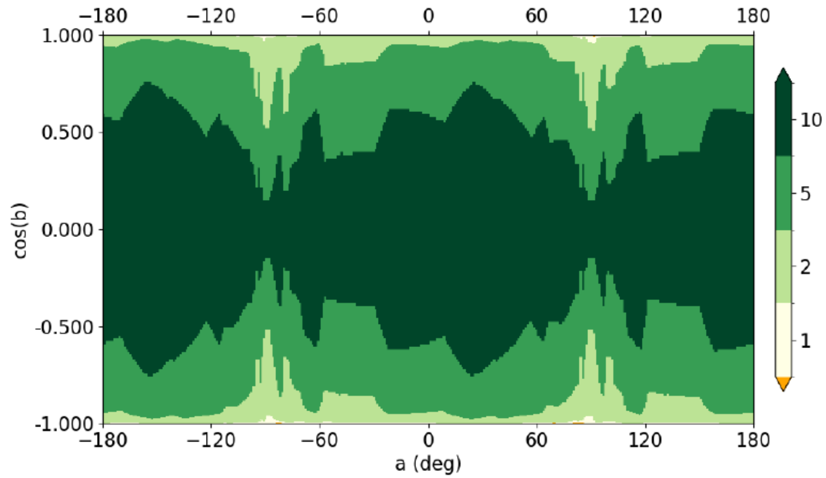

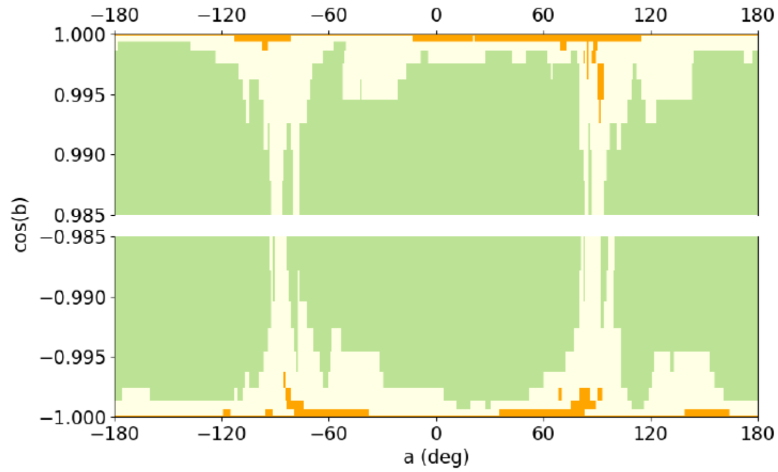

Top − the exclusion regions of the directional parameters, *a* and cos(*b*), of the mirror-magnetic-field vector corresponding to the limit curves. Bottom − zoom-in to the solid angle regions at values $|\cos(b)|-1 < 10^{-4}$, where the anomalous signals were not excluded (orange on the scale).

Finite splitting: resonant n → n′ conversion

Non-relativistic Hamiltonian; possible hidden-sector potentials are absorbed into the generalized δm

$$H = \begin{pmatrix} m_n + V & \varepsilon_{nn'} \\ \varepsilon_{nn'} & m_n + \delta m \end{pmatrix} \qquad P^{nn'}(t) = \frac{1}{\tau_{nn'}^2 \left(\frac{V-\delta m}{2\hbar}\right)^2} \sin^2\left(\frac{V-\delta m}{2\hbar} t\right)$$

Experimental observable: asymmetry from two magnetic field settings

$$A_{ij} = \frac{n_i - n_j}{n_i + n_j} = \frac{\exp(-m_s P_i^{nn'}) - \exp(-m_s P_j^{nn'})}{\exp(-m_s P_i^{nn'}) + \exp(-m_s P_j^{nn'})}$$

Time constant and limit from MCUCN simulations in inhomogeneous field

$$\tau_{nn'} = \frac{1}{\sqrt{2|\langle A_{ij}\rangle|}} \sqrt{|F(B_i, \delta m) - F(B_j, \delta m)|}$$

H0 hypothesis testing of anomalies

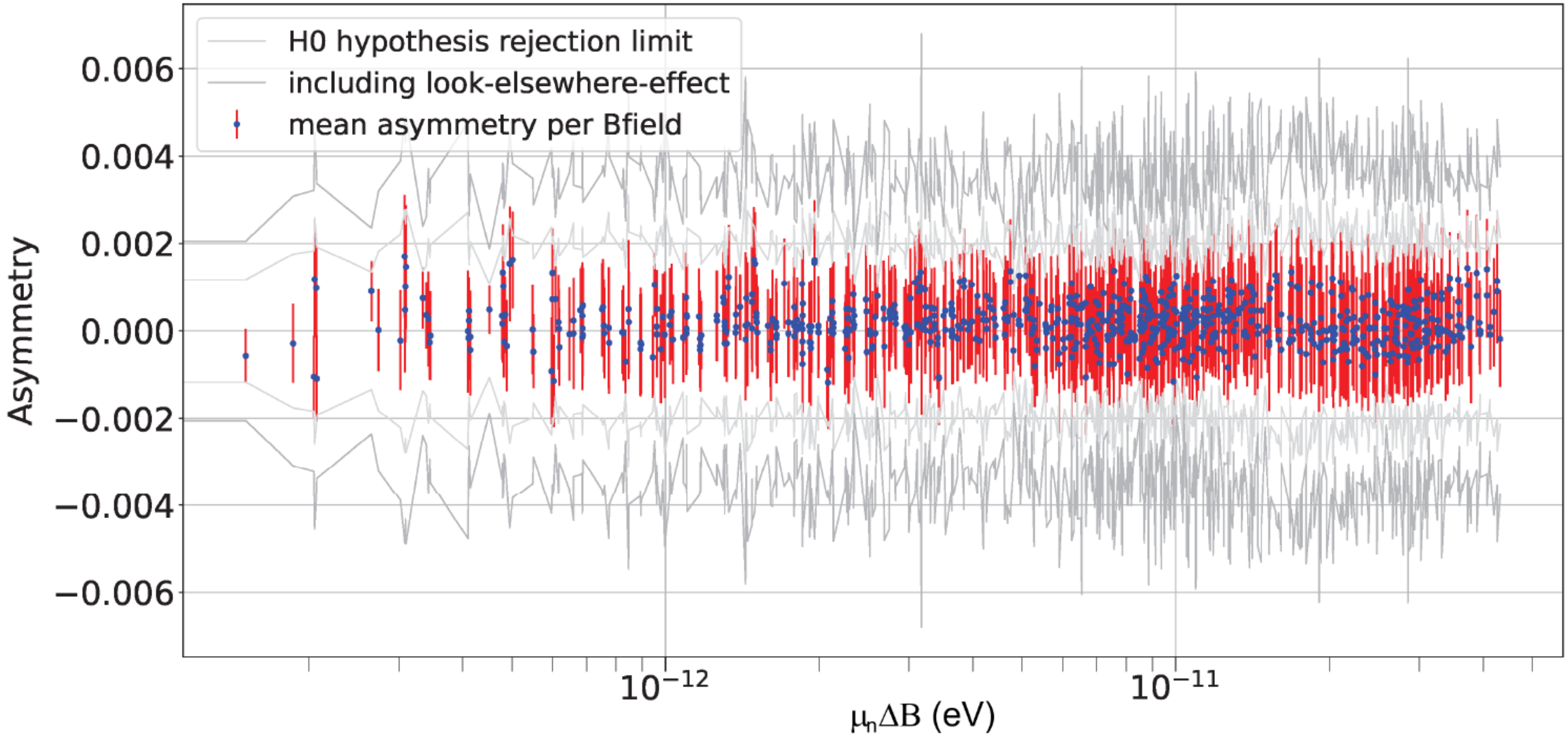

Mean asymmetry $\langle A_{i,j} \rangle$ as a function of the magnetic field differences converted into energy unit. The light grey line shows the limits of the null-hypothesis H0 at 95% C.L., the dark grey outline shows the same limit after correcting for the look-elsewhere-effect. $\langle A_{i,j} \rangle$ is consistent with H0 within a standard error $\delta \langle A_{i,j} \rangle$.

Limits for a finite generalized splitting

Zoom: peV range

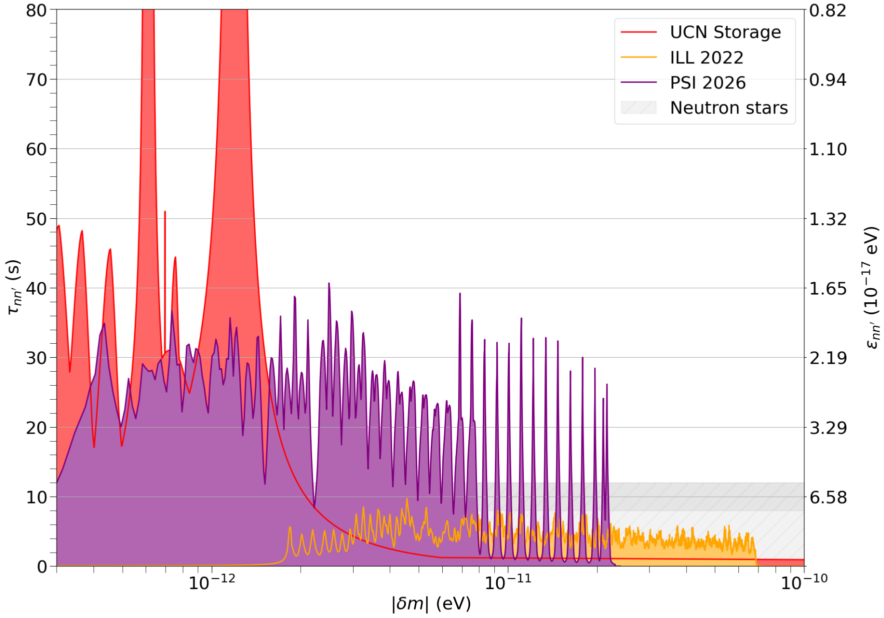

Extended comparison

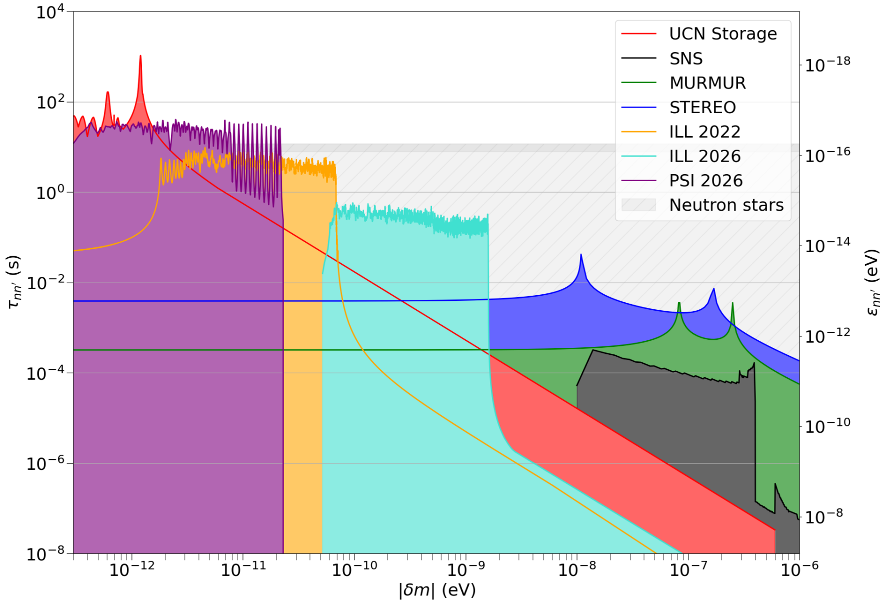

PSI 2026 (purple): the limits reach $\tau_{nn'} \simeq 20$ s over parts of 0.3–22 peV and become more stringent than the model-dependent neutron-star estimate in part of this interval. The extended comparison includes the updated ILL 2026 and SNS results.

N. J. Ayres et al., "Laboratory constraints on peV-scale mass splitting between ordinary and sterile neutron states," arXiv:2608.12173v2 (2026), Fig. 4.

Conclusions

- Mirror matter is a Standard-Model-like, self-interacting dark sector. Neutron mixing offers a direct laboratory test of a possible connection between the ordinary and mirror sectors.
- **Exact-mirror benchmark:** previously claimed B′-dependent UCN loss anomalies in the 5–109 μT range are excluded at 95% C.L. over 99.98% of the 4π directions.
- **Beyond exact mirror parity:** n′ need not have the neutron mass. The finite-splitting search reaches $\tau_{nn'} \simeq 20$ s over parts of 0.3–22 peV.
- UCN experiments therefore probe both a specific mirror-neutron model and more general hidden or sterile neutron states.

N. J. Ayres et al., Phys. Rev. Lett. 137, 051802 (2026); N. J. Ayres et al., arXiv:2608.12173v2 (2026).

Thank you!